Structural Strength Analysis of 57-Ton Capacity Flat Carriage Coal Transporter with 2x20 Feet Container Subjected to Operation Conditions

Gozali, Muchamad
PRTKS, National Research and Inovation Agency

Nuramin, Makmuri
PRTKS, National Research and Inovation Agency

Djoko Wahyu Karmiadji
PRTKS, National Research and Inovation Agency

Sulistiyo, Wahyu
PRTKS, National Research and Inovation Agency

他

https://doi.org/10.5109/7151770

出版情報：Evergreen. 10 (3), pp.2029-2037, 2023-09. 九州大学グリーンテクノロジー研究教育センター
バージョン：

Structural Strength Analysis of 57-Ton Capacity Flat Carriage Coal Transporter with 2x20 Feet Container Subjected to Operation Conditions

Muchamad Gozali[1], Makmuri Nuramin[1*], Djoko Wahyu Karmiadji[1,2], Wahyu Sulistiyo[1], Hedi Purnomo[3]

[1]PRTKS, National Research and Inovation Agency, Indonesia

[2]Department of Mechanical Engineering, Universitas Pancasila, Indonesia

[3]The Indonesian of Rail Road Industry, Indonesia

*E-mail: makm001@brin.go.id

(Received May 10, 2023; Revised July 29, 2023; accepted August 18, 2023).

Abstract: A flat carriage is a vehicle type without a body and a roof for transporting goods, designed to meet the needs of heavy goods. Several conceptions are elaborated, with respect to capacity of 57-ton recommended to 2x20 feet containers. The aim of the paper follows determining the strength and durability of the flat carriage under operational loading at accordance with the required criteria and using a fatigue limit diagram approach based on the Soderberg method. This research was conducted with static and dynamic tests. The sections for 50 strain gauges were indicated based on data from to the finite element method. The results showed that in the case of vertical static loading, the maximum stress on the flat carriage structure occurred at full vertical load (50,050 kg) in the end centre sill area, at single measuring location no. 24, with a value of 59.8 MPa, and the results of the static test were still below the allowable stress of the material at 243.8 MPa. Meanwhile, at the dynamic loading conditions, the greatest stress occurred at single measuring location no. 24 with mean stress value of 59.7 MPa, stress amplitude was 17.8 MPa, and at single measuring location no. 23 with mean and stress amplitude values of 59.6 MPa and 34.4 MPa, respectively. The results of the analysis showed that the mean stress value (σ_{mean}) and amplitude stress value (σ_{amp}) were still below the fatigue limit curve of the Soderberg diagram. From the results of this research, it was concluded that the 57-ton flat carriage prototype construction/structure, under static and dynamic loads, can be manufactured as many as operational needed.

Keywords: prototype; flat carriage; stress; Soderberg diagram.

1. Introduction

Flat wagon has a strategic role in serving distribution by coal transports in Indonesia, especially in the railway lines of Java and Sumatra[1–4]. The role of flat carriages in the logistics of transporting coal, is to enable transport of large quantities efficiently, cheaply, regularly, scheduled, reliably and safely, with a low environmental impact[5–7]. Different types of flat carriage are developed according to the type of goods to be transported. Studies related to the research through mathematical modeling with dynamic loading on a flat carriage transport structure to transport military equipment such as a tank with a combat load of 55 tons are prototyped[8–11].

One type of flat wagon that underwent a new structural design on the lower frame was the flat carriage for transporting coal in a 2x20 ft container, with a maximum load capacity value of up to 57-ton[12]. In its operation, the coal-transporting flat carriage experiences various static and dynamic loads on its structure, due to the condition of the railroad that could be straight, turns left or right, go uphill and downhill; and at the time of stopping, when there is braking, experiencing compression to the structure due to the series of carriages from the front-rear. The impact of these operational loading conditions could affect the structure/ construction of the carriage[13–16]. The Indoneian regulation of the Minister for Transportation number PM 17 of 2011 states that every carriage operated must have the structural strength and durability in receiving operational loading[17]. The purpose of this study is focused on determination of the structural strength and durability of the 57-ton flat wagon prototype at operational conditions, in accordance with the specified acceptance criteria, and to use a fatigue limit diagram approach to the relationship between the mean stress and

stress amplitude based on the Soderberg method[13,17,18].

2. Coal Transportation

Increasing energy consumption by industrial developing countries, it becomes difficult to maintain coal supplies. Therefore, it needs the development of technology to utilize coal, improvement of environmental and operational performance as well as fuel diversification for coal-fired power plants[19–21]

The transportation of coal using the South Sumatra 57-ton flat carriage (Gerbong Datar or GD), is a form of cooperation between PT Kereta Api Indonesia and PT Bukit Asam Tbk, PT Semen Baturaja Tbk, PT Bara Alam Utama, PT Bara Multi Sugih Sentosa and PT Gumay Prima Energy, in meeting domestic needs and also exports to several countries[20,22,23]. The process of coal loading is carried out at Suka Cinta Station, Lahat Regency, South Sumatra, then transported to Kertapati Palembang Station, South Sumatra which has access to the port (Figure 1).

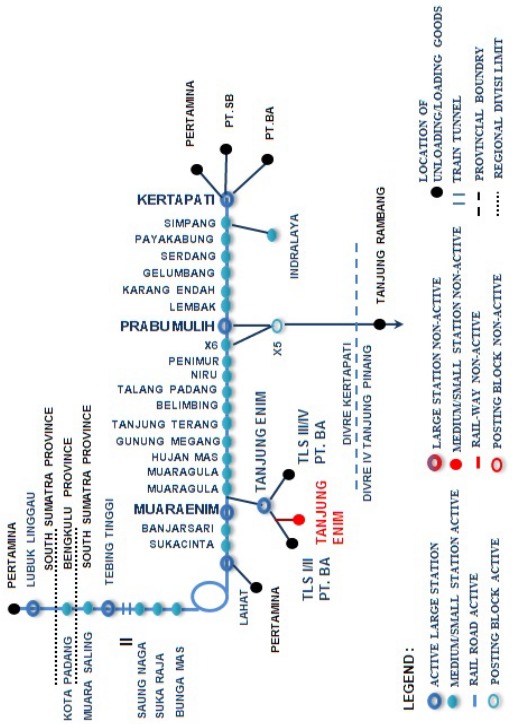

Fig. 1: Existing railway lines for transporting coal in South Sumatra

3. Material and Methods

3.1 Material

The object of this study is a prototype of the 57-ton flat wagon, which is used to transport coal in a 2x20 ft container (Figure 2 and 3). This prototype or test object was a product of PT. Industri Kereta Api (INKA), Madiun[24,25]. Here are the technical data of the 57-ton flat wagon test piece[26,27]:

a) maximum load capacity (carrying capacity): 57 tons
b) maximum empty weight: 15 tons
c) design speed (maximum): 80 km/h,
d) operational speed: 75 km/h,
e) rail width: 1,067 mm
f) carriage base frame length: 12,495 mm
g) carriage width: 2,438 mm.

Fig. 2: 57-ton flat trolley Prototype

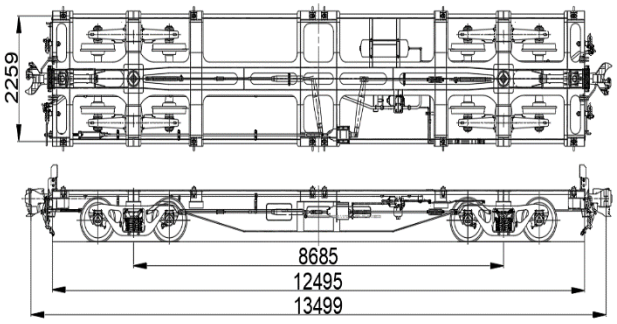

Fig. 3: Technical drawing of 57-ton flat wagon

The main structural parts of the 57-ton flat wagon observed in this study were the lower structures on the center sill, side sill, cross beam and bolster that were built with a welding system by using steel grades of SM 490 and SM 570 (JIS G3106) equivalent to A572 and A913 Gr65 (ASTM); S355JR and S460M (EU). The material specifications and chemecal compositions are shown in Table 1 and 2 respectively.

Table 1. Mechanical properties[28]

Material	Yield stress (MPa)	Ultimate tensile stress (MPa)	Position
SM490	325	490	Side sill
SM570	460	570	Center Sill

Table 2. Chemical compositions[29]

Symbol of Grade	SM490	SM570
C	0.22 %	0.18 %
Si	0.55 %	0.55 %
Mn	1.60 %	1.60 %
P	0.035 %	0.035 %
S	0.035 %	0.035 %

3.2 Methods

The methods used in measuring the strength of the 57-ton GD structure were[30–32]:

a. Simulating finite element method of 57-ton GD construction design / structure.
b. Static and dynamic tests to the 57-ton GD prototype under coal operational load, with 2x20 ft containers.

3.3. Finite Element Simulation

Before the testing was conducted, the 57-ton GD test object was simulated using finite element method to determine critical areas of the bogie structure and, at the same time, to determine the magnitude of the stress that occurs in its structure. These stress estimation and analysis were obtained using numerical simulations of finite element methods. Simulation was carried out by conditioning the test object as it was when in operating conditions. The first step in simulating the finite element method was to make the geometry uses plate elements. From the existing geometry, the boundary condition was determined according to the actual condition of the test object when in operation. The dynamic factor was calculated as its actual load multiplier according to the standards used. Flat carriages used a dynamic factor value of 1.3 according to EN 12663 of 2010[19,24,33,34]. Geometry modelling with finite element simulation method was divided into 2 parts, i.e. the center sill section, the most critical part of the flat carriage, and the side sill with crossbeam sections as shown in Figure 4,5, and 6. The forces on the flat carriage test object were adjusted to the conditions, when the load is given due to a 2x20 ft container through 8 contact points between the container and flat carriage. The results of simulation can be indentified that the highest stress is 143,5 Mpa located at the bottom plate of the center sill. This value is less than 345 MPa or allowable stress value of SM570 material as seen in Figure 7 and 8. In the 2nd area of side sill and cross beam can be identified that the maximum allowable stress value is 206.6 Mpa and less than 243.7 Mpa as the value of SM490 material as seen in Figure 9 and 10.

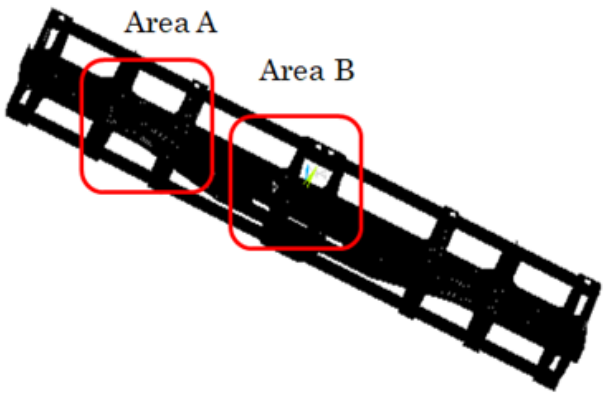

Fig. 4: Finite element model

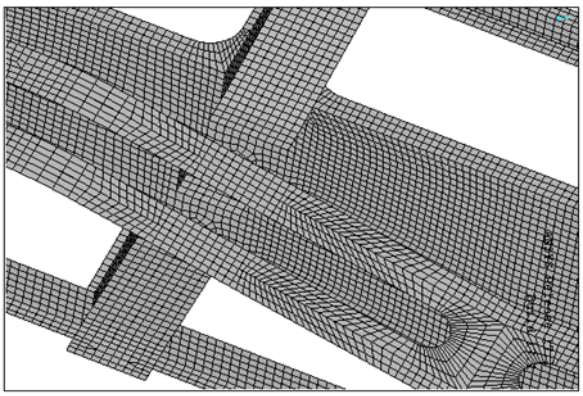

Fig. 5: Detail meshing area A

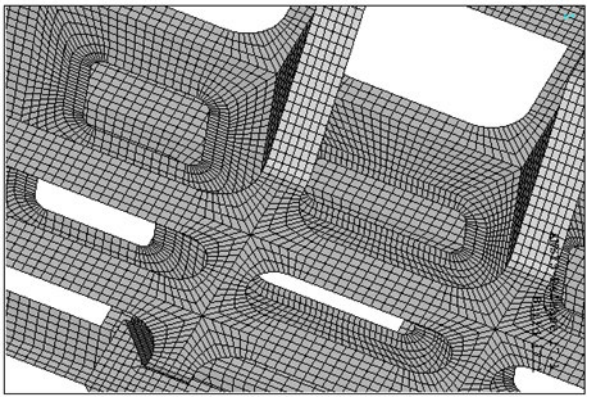

Fig. 6: Detail meshing area B

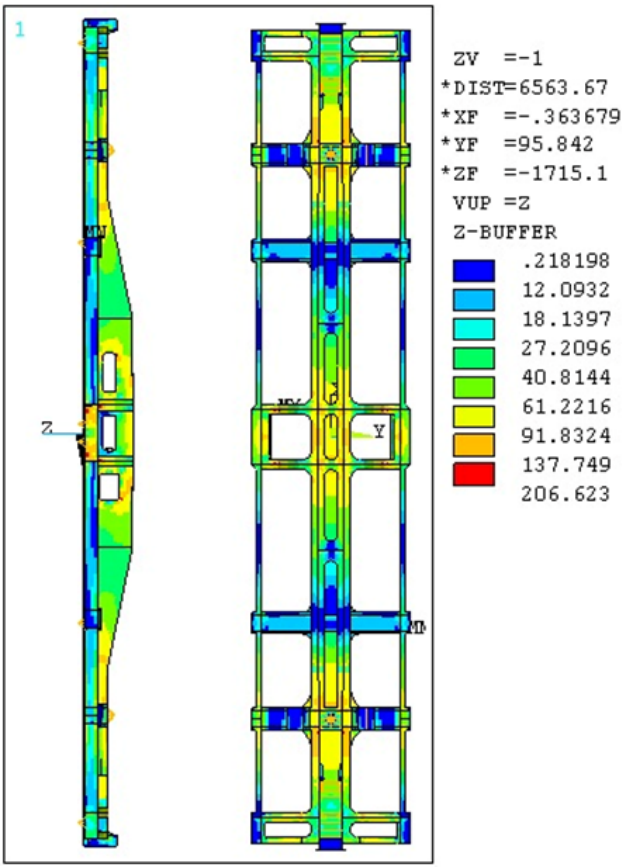

Fig. 7: Simulation results of sub case 1 57-ton GD, load by 2x20 ft container

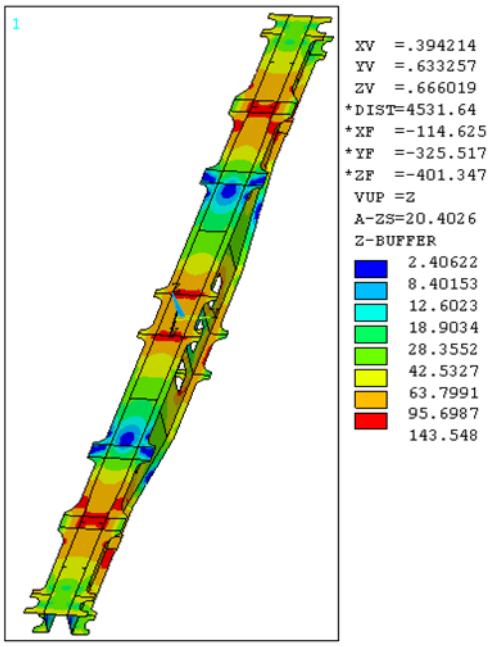

Fig. 8: Simulation results of sub case 1 57-ton flat wagon, load by 2x20 ft ISO container, SM570 material

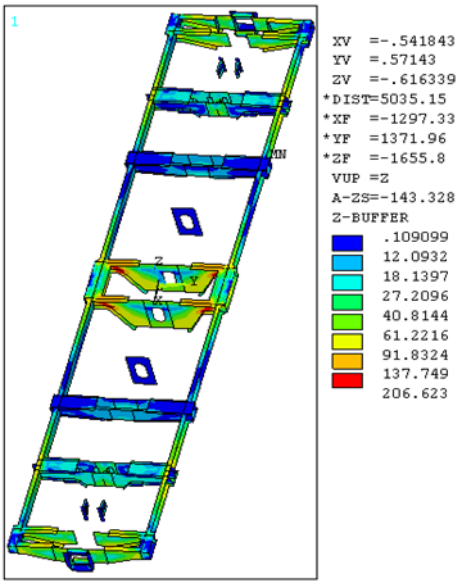

Fig. 9: Simulation results of sub case 1 57-ton flat wagon, load by 2x20 ft ISO container, SM490 material

To validate the stress values resulted from the simulation finite element method, 50 strain gauges were installed at various location in the critical point of the test object in accordance with the FEM analysis i.e. in the bottom plate center sill area and the side sill and cross beam areas and measured during the dynamic testing[32].

The single type strain gauge was used when the strain gauge direction and the condition of the strain gauge placement point were detected laterally or longitudinally, and rosette type strain gauge was used when the strain direction and placement position of the strain gauge show more than one direction such as near the radius and others.

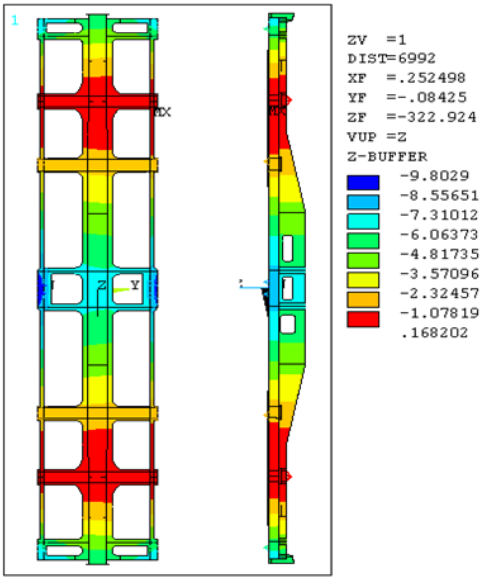

Fig. 10: Simulation results of sub case 1 57-ton GD, load by 2x20 ft ISO container, SM490 material

Figure 11 shows sketch of strain gauge location due to FEM stress analysis on 57-ton GD, and Figure 12 shows the example of the strain gauge installation on 57-ton flat wagon test object.

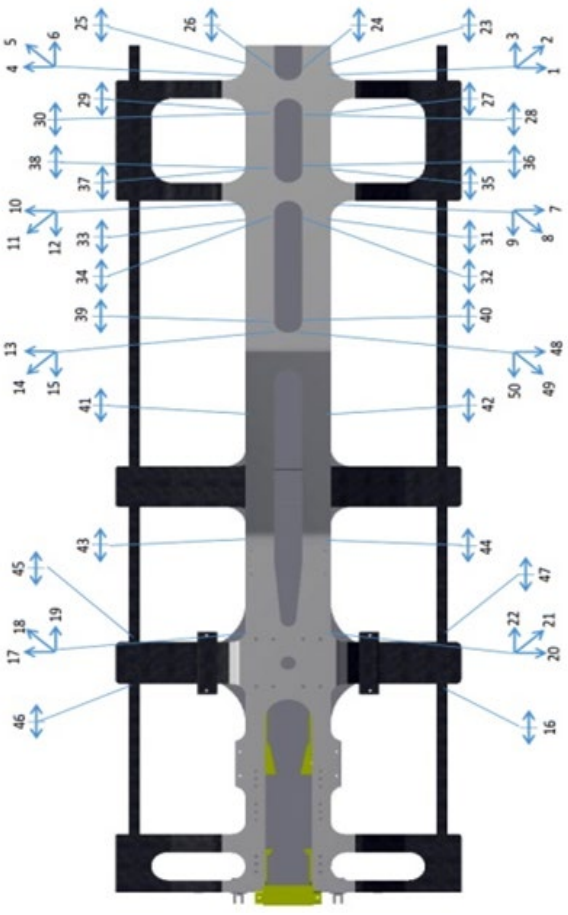

Fig. 11: Location of strain gauge on 57-ton GD

Fig. 12: Strain gauge installation on 57-ton flat wagon

The experiment was carried out through static and dynamic testing of 57-ton GD along with an operating load of coal in a 2x20 ft container. The goal is to find out the strength and durability of the carriage in receiving operational loading according to the specified acceptance criteria and use the fatigue limit diagram approach based on the Soderberg method[13,35].

The test object or 57-ton GD prototype with a serial number GD 54 15 725 having 50 pieces of strain gauge sensors mounted according to the result of finite element analysis was tested by using static and dynamic loading. The locations of strain gauge on the specimen are shown in Figure 11 in the areas of center sill, side sill and bolster.

The 57-ton GD test specimen was attahed to the locomotive, other coal-carrying GDs and also passenger cars along with the measuring equipment. Figure 13 shows one of passenger car equipped data acquisition systems to measure strain values for static and dynamic testing. The experiment was executed by using the 46 channel Deicy DR-600 system data acquisition.

Fig. 13: Test car and data acquisition system to measure strain for static and dynamic testing.

3.4. Wagon Dynamic Test

Static load testing in this study was carried out when the 57-ton GD prototype test object stopped at Suka Cinta Station, Lahat Regency, with the following steps:

a) before loading the tested object
b) the condition of the test object with empty load of container-1 20 ft.
c) the condition of the tested object with empty load of container-2 20 ft.
d) the coal load is fed into container-1 and container-2 gradually up to the maximum load (20 backhoes), where each container is filled 10 backhoes.

The strain is measured in each step and recorded as strain data. Loading process to the 2x20 ft container along with coal is shown in Figure 14.

Weighing the container and coal loads should be done and the result can be described as the following data:

a) Container weight 1 = 3 tons, weight of coal on container 1 = 22660 kg
b) Container weight 2 = 3 tons, weight of coal on container 2 = 22050 kg
c) The full load value for the 2x20 ft container was 50710 kg.

Fig. 14: The loading process of container and coal.

The dynamic experiment was carried out by pulling the 57-ton GD under full load condition, followed by the series of other coal-carrying GDs and the locomotive train as prime mover. This series of coal transporting GD carriages runs through the coal transportation distribution line of South Sumatra, starting from Suka Cinta Station, Lahat Regency to Kertapati Palembang Station, South Sumatra, see Figure 1. Measurements were made in real-time when this series of coal carrier GDs was moving (operating). The test results were in the form of strain data recorded in real-time. Given the capacity of the measuring instrument, measurements were not carried out continuously along the travel route above, but were carried out in several conditions[36–38], i.e. when the track in condition of straight railway, sharp right turn, long left turn and straight turn railway

3.5. Acceptance Criteria

The acceptance criterion in the 57-ton GD static test was that the strain value of GD structure should not exceed 75% of the material's yield stress (< 75% yield strength)[34].

Table 3. Criteria for acceptance of material 57-ton flat wagon

Material	Allowable Stress [0.75*Yield Stress]	Allowable Strains [0.75*Yield Strains]
SM490	243,75 MPa	1177,5 με
SM570	345 MPa	1666,7 με

4. Result and Discussion

4.1. Evaluation of Static Test Results

To evaluate its stress value, the measured strain was converted to stress value. There were two types of strain sensors used for measurements, namely *the single* type and the rosette type with an angle of 45°/90°, see Figure 16[13,39]. The relationship between strain and stress for the *single* strain sensor type can be expressed by Hooke's law as formulated in the Equation. (1) as follows.

$$\sigma = \varepsilon E \quad (1)$$

For the rosette strain gauge type with an angle of 45°/90°, Equation. (2) and (3) can be used[13]:

$$\sigma_{1,2} = \frac{E}{2}\left[\left(\frac{\varepsilon_a+\varepsilon_c}{1-\nu}\right) \pm \frac{\sqrt{2}}{1+\nu}\sqrt{(\varepsilon_a-\varepsilon_b)^2+(\varepsilon_b-\varepsilon_c)^2}\right] \quad (2)$$

$$\sigma_{1,2} = \frac{E}{1.4}\left[(\varepsilon_a+\varepsilon_b) \pm 0.76\sqrt{(\varepsilon_a-\varepsilon_b)^2+(\varepsilon_b-\varepsilon_c)^2}\right] \quad (3)$$

Meanwhile, the equivalent stress value was obtained by calculation based on the Huber - Von Mises – Hencky criterion, in which the criterion is still analyzed by a lot of research groups[40–42].

$$\sigma_{eq} = \sqrt{\sigma_1^2+\sigma_2^2-\sigma_1\sigma_2} \quad (4)$$

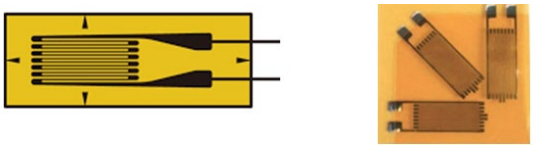

Fig. 15: Strain gauge sensor configuration for single (10 mm x 6 mm), and rosette 45°/90°(Figure 12)[43]

The static test results were in the form of strain measurement data which were converted into stress values by equation (1), (2) and (3), the strain and the stress values were evaluated with the requirements specified in its acceptance criteria. Table 3 indicates the strain and the greatest stress value at the static loading results, The largest strain was occurred at the full vertical loading, at the location of the measuring point 10, 11, 12 (rosette) with the maximum strain result ε_a = -209.6 µm /m, ε_b = 61.2 µm /m, ε_c = 344.0 µm/m. Using equation (3) to obtain the main stress of $\sigma_{1,2}$ for the rosette strain is σ_1 = 63.9 MPa, and σ_2 = **24.1** MPa. Meanwhile, based on equations (3) and (4), for the rosette strain gauge, an equivalent stress value of **78.8** MPa was obtained.

For the use of equation (1), as an example for the test result with load of 2 empty containers, the largest strain was obtained in the single strain gauge type, i.e. a maximum strain of **91.6** µm/m. Using equation (1), a stress value was obtained for a single strain gauge σ = **18.9** MPa.

4.2. Evaluation of Dinamic Test Results

The dynamic strength of the GD 57-ton structure was determined based on the fatigue life of the material used. To avoid failure, the stress due to cyclic loading should not exceed the fatigue limit of the material. One method of analyzing the fatigue of metal structures was the fatigue limit diagrams approach. The fatigue limit diagram is a diagram that illustrates the relationship between the mean stress and the stress amplitude, both parameters affect metal fatigue. The fatigue limit diagram methods commonly used were Soderberg (Equation 5), Goodman (Equation 6), Gerber (Equation 7), and Morrow (Equation 8) that are explored in the curve in Figure 17[25]. The symbol are the limit of fatigue strength (S_e) on the ordinate axis of the alternating stress amplitude (σ_a) to yield strength (S_y), ultimate strength (S_u), or fracture or fatigue strength (σ_f), on the abscissa axis of average stress (σ_m).

$$\text{Soderberg} \rightarrow \frac{\sigma_a}{S_e}+\frac{\sigma_m}{S_y}=1 \quad (5)$$

$$\text{Goodman} \rightarrow \frac{\sigma_a}{S_e}+\frac{\sigma_m}{S_u}=1 \quad (6)$$

$$\text{Gerber} \rightarrow \frac{\sigma_a}{S_e}+\left(\frac{\sigma_m}{S_u}\right)^2=1 \quad (7)$$

$$\text{Morrow} \rightarrow \frac{\sigma a}{Se}+\frac{\sigma m}{Sf}=1 \quad (8)$$

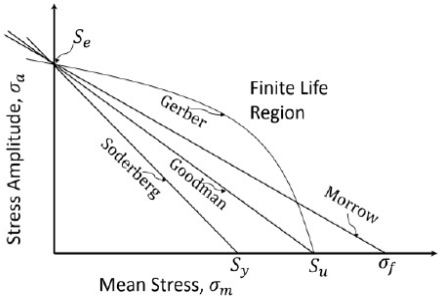

Fig. 16: Fatigue limit diagram

The Søderberg method was the most conservative and safest method to obtain the fatigue safety criteria, according to the curve of the stress function in Figure 16. This consideration was based on the 57-ton GD structure materials i.e., SM 490 and SM 570 steels, where the theoretical resistance/fatigue limit of the steel is 1/2 of the ultimate tensile strength. The structure is said to be safe from damages due to fatigue of Huber – Von Mises – Hencky, if the combination of mean stress and stress amplitude that occurs due to the loading, is below the fatigue limit line. Meanwhile, if the stress that occurs is above the fatigue limit line, the structure will be damaged due to cyclic loading. From the strain measurement results data, the maximum stress, minimum stress, mean stress, and stress amplitude were determined. The relationship between maximum stress (σ_{max}), minimum stress (σ_{min}), mean stress (σ_{mean}), and stress amplitude (σ_{amp}) is expressed by the following equation[13,18].

To obtain the stress values that will be used to perform the fatigue analysis, equations 1,2 and 3 above were used. The results of stress value calculation based on the strain

data from the dynamic test, are shown in Table 4. The table presents data on mean stress (σ_{mean}), and the stress amplitude (σ_{amp}) in several railway condition, the straight railway measurement is about 10 km and the number of each left and right turn about 5 time consecutively. Table 5 is only a part of the data that contains measurement data on some railway conditions, not all data is presented, only the largest stress data.

Table 4. The maximum strain and stress values at static loading tests

Load conditions	*Maximum*					
	Strain gauge no	***SG Type***	$\varepsilon_a\ \varepsilon_b\ \varepsilon_c$ **(μ)**	$\sigma_a\ \sigma_b\ \sigma_c$ **(MPa)**	$\sigma_{1,2}$ **(MPa)**	σ_{eq} **(MPa)**
Empty load (without containers)	10,11, 12	Rosette	10.4 8.4 9.2	2.2 1.7 1.9	3.0 2.7	3.0
Load 1 empty container	29	Single	39.2	8.1	-	8.2
Load 2 empty containers	29	Single	91.6	19.0	-	19.2
Full vertical load	10,11, 12	Rosette	-209.6 61.2 344	-43.4 12.7 71.2	63.9 -24.1	78.8

Table 5. Values of amplitude and mean level of stress

Strain Gauge number	**Straight railway**		**Sharp right turn**		**Long left turn**		**Stright turn railway**	
	σ_{mean}	σ_{amp}	σ_{mean}	σ_{mean}	σ_{amp}	σ_{amp}	σ_{mean}	σ_{amp}
	MPa	**MPa**	**MPa**	**MPa**	**MPa**	**MPa**	**MPa**	**MPa**
7, 8, 9	66.6	22.5	72.5	22.3	87.2	29.2	103.3	21.6
10, 11, 12	84	21.9	79.1	67.5	29.0	23.4	67.5	29.0
16	43.4	41.0	53.6	50.7	37.5	31.2	50.7	37.5
24	46.3	76.7	55.2	59.2	58.7	60.0	59.2	58.7
25	73.0	34.2	73.5	74.6	27.4	30.5	74.6	27.4
26	62.0	78.5	55.3	53.4	59.7	61.4	53.4	59.7

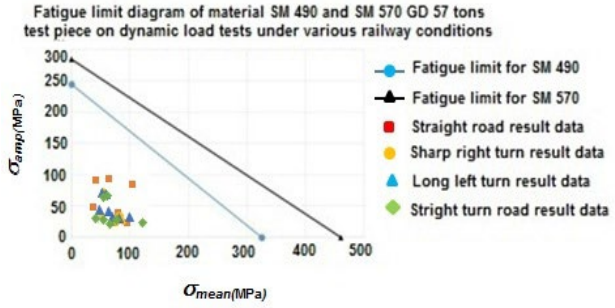

Fig 17. Fatigue limit diagram of material SM 490 and SM 570 GD 57-ton test piece on dynamic load tests under various railway conditions[43,44].

The evaluation data in the form of mean stress values (σ_{mean}), and stress amplitude (σ_{amps}), were plotted against the Soderberg method fatigue limit diagram for SM 490 and SM 570 materials, as shown in Figures 17. Figure 17 show data from railway conditions that depict and represent the condition of the 57-ton GD railroad on the island of Sumatra, especially the railway line from Suka Cinta Lahat Station to Kertapati Palembang Station.

5. Conclusion

Based on the experiment results and discussion, it can be summarized as follows:

1. Under the condition of 2x20 ft static load, all stress values that occurred were below the allowable stress or have met the requirements of the specified acceptance criteria.
2. When the experiment was running on static loading with the condition of full load (50710 kg), the highst stress values are occurred and shown in table 4, at the Rosette measuring point of 10, 11, 12 with σ_{eq} = 78.8 MPa, in which this value is far below the material's allowable stress of 345 MPa.
3. From the Table 5 the highest mean stress (σ_{mean}) is 103.34 MPa, and the highest stress amplitude (σ_{amps}) is 78.49 MPa.
4. In the dynamic load tests (on the track test), all stress values do not exceed the fatigue limit material.

The summary of experiment and discussion can be summarized that the 57-ton GD prototype structure fulfills the specified acceptance criteria. The additional criteria include safe from damages due to fatigue failure, the requirements of the Minister of Transportation of the Republic of Indonesia No. PM 17 of 2011, and also suitable to use for coal transportation purposes with a planned maximum capacity of 57 tons.

Acknowledgments

The authors would like to thanks to National Research and Innovation Agency and PT. Industri Kereta Api Madiun for funding and collaborated in this research

Nomenclature

σ	*Stress* (MPa),
ε	*Strain* (με),
E	Young's modulus (MPa).
$\sigma_{1,2}$	main stress with σ_1 and σ_2 (MPa) direction.
ν	Poison's ratio
ε_a	Strain in the horizontal direction of 0°
ε_b	Strain in the 45° direction
ε_c	Strain in the vertical direction of 90°

References

1) A.E. Bempong, "The role of transportation in logistics chain," *Texila Int. J. Manag.*, **5** (*1*) 147–161 (2019). doi: 10.21522/tijmg. 2015.05.01.art015.
2) H. Dwiatmoko, D. Supriyatno, and S.W.

Mudjanarko, "The role of railway infrastructure development on the regional economic growth," *Int. J. Sustain. Constr. Eng. Technol.*, **11** (*1*) 125–135 (2020).
3) T. Junaedi, "Forecasting of freight demand transportation (case study in lampung province, indonesia)," *IOP Conf. Ser. Mater. Sci. Eng.*, **1232** (*1*) 012008 (2022). doi:10.1088/1757-899x/1232/1/012008.
4) S.M. Utomo, B.A. Nugroho, T.W. Sasongko, and A. Krisnowo, "Competitiveness analysis railway propulsion system industry in indonesia - pre feasibility study," *Int. J. Adv. Eng. Res. Sci.*, **7** (*5*) 324–332 (2020). doi:10.22161/ijaers.75.40.
5) S. Jansuwan, A. Chen, and X. Xu, "Analysis of freight transportation network redundancy: an application to utah's bi-modal network for transporting coal," *Transp. Res. Part A Policy Pract.*, **151** (*July 2019*) 154–171 (2021). doi:10.1016/j.tra.2021.06.019.
6) M. Darayi, K. Barker, and C.D. Nicholson, "A multi-industry economic impact perspective on adaptive capacity planning in a freight transportation network," *Int. J. Prod. Econ.*, **208** 356–368 (2019). doi:10.1016/j.ijpe.2018.12.008.
7) M. Milenković, N. Bojović, and D. Abramin, "Railway freight wagon fleet size optimization: a real-world application," *J. Rail Transp. Plan. Manag.*, **26** (*January*) 100373 (2023). doi:10.1016/j.jrtpm.2023.100373.
8) V. Stoilov, S. Slavchev, V. Maznichki, and S. Purgic, "Analysis of some problems in the theoretical wagon strength studies due to the imperfection of the european legislation," *IOP Conf. Ser. Mater. Sci. Eng.*, **618** (*1*) (2019). doi:10.1088/1757-899X/618/1/012045.
9) O. Fomin, J. Gerlici, A. Lovska, and K. Kravchenko, "Analysis of the loading on an articulated flat wagon of circular pipes loaded with tank containers," *Appl. Sci.*, **11** (*12*) 1–12 (2021). doi:10.3390/app11125510.
10) A. Reidemeister, L. Muradian, V. Shaposhnyk, O. Shykunov, O. Kyryl'chuk, and V. Kalashnyk, "Improvement of the open wagon for cargoes which imply loading with a 'hat,'" *IOP Conf. Ser. Mater. Sci. Eng.*, **985** (*1*) (2020). doi:10.1088/1757-899X/985/1/012034.
11) O. Fomin, G. Vatulia, and A. Lovska, "Loading on the carrying structure of a flat wagon when transporting firing military equipment," *IOP Conf. Ser. Mater. Sci. Eng.*, **1002** (*1*) (2020). doi:10.1088/1757-899X/1002/1/012012.
12) N.S. Zulkefly, H. Hishamuddin, F.A.A. Rashid, N. Razali, N. Saibani, and M.N.A. Rahman, "The effect of transportation disruptions on cold chain sustainability," *Evergreen*, **8**(*2*) 262–270 (2021). doi:10.5109/4480702.
13) D.W. Karmiadji, M. Gozali, A. Anwar, H. Purnomo, M. Setiyo, and R. Junid, "Evaluation of operational loading of the light-rail transit (lrt) in capital region, indonesia," *Automot. Exp.*, **3** (*3*) 104–114 (2020). doi:10.31603/ae.v3i3.3882.
14) O. Fomin, J. Gerlici, G. Vatulia, A. Lovska, and K. Kravchenko, "Determination of the loading of a flat rack container during operating modes," *Appl. Sci.*, **11** (*16*) (2021). doi:10.3390/app11167623.
15) F. Oleksij, L. Alyona, R. Valentyna, H. Anatoliy, S. Inna, and G. Olga, "The dynamic loading analysis of containers placed on a flat wagon during shunting collisions," *ARPN J. Eng. Appl. Sci.*, **14** (*21*) 3747–3752 (2019).
16) O. Fomin, J. Gerlici, A. Lovskaya, M. Gorbunov, K. Kravchenko, P. Prokopenko, and T. Lack, "Dynamic loading of the tank container on a flat wagon considering fittings displacement relating to the stops," *MATEC Web Conf.*, **234** (2018). doi:10.1051/matecconf/201823405002.
17) M. for transportation republic of Indonesia, "Peraturan menteri perhubungan nomor : pm. 17 tahun 2011 tentang standar, tata cara pengujian dan sertifikasi kelaikan gerbong (Minister for transportation regulation number: pm. 17 of 2011 concerning standards, procedures for testing and certifying the el," 2011.
18) D.W. Karmiadji, B. Haryanto, O. Ivano, M. Perkasa, and R. Abdul Farid, "Bogie frame structure evaluation for light-rail transit (lrt) train: a static testing," *Automot. Exp.*, **4** (*1*) 36–43 (2021). doi:https://doi.org/10.31603/ae.4252.
19) Q.H. Phung, K. Sasaki, Y. Sugai, M. Kreangkrai, T. Babadagli, K. Maneeintr, and B. Tayfun, "Numerical simulation of co2 enhanced coal bed methane recovery for a vietnamese coal seam," *J. Nov. Carbon Resour. Sci.*, **2** 1–7 (2010). http://scholar.google.com/scholar?hl=en&btnG=Search&q=intitle:Numerical+Simulation+of+CO+2+Enhanced+Coal+Bed+Methane+Recovery+for+a+Vietnamese+Coal+Seam#0.
20) B. Sulistianto, T. Karian, Kardiansyah, S. Hidayatullah, and S. Widhy, "Optimalization of outpit dump at asam-asam open pit coal mine , pt arutmin indonesia," *J. Nov. Carbon Resour. Sci.*, **7** 53–59 (2013).
21) S. Nozawa, N. Wada, Y. Matsushita, T. Yamamoto, M. Omori, and T. Harada, "Experimental and numerical investigation of effect of coal rank on burn-off time in pulverized coal combustion," *J. Nov. Carbon Resour. Sci.*, **5** (*2*) 23–27 (2012).
22) P. Pradono, I. Syabri, Y.R. Shanty, and M. Fathoni, "Comparative analysis on integrated coal transport models in south sumatra," *J. Environ. Treat. Tech.*, **7** (*4*) 696–704 (2019).
23) J. Sherwood, R. Bickhart, E. Murawski, Z. Dhanani, B. Lytle, P. Carbajales-Dale, and M. Carbajales-Dale, "Rolling coal: the greenhouse gas emissions of coal

rail transport for electricity generation," *J. Clean. Prod.*, **259** 120770 (2020). doi:10.1016/j.jclepro.2020.120770.
24) O. Fomin, J. Gerlici, A. Lovskaya, K. Kravchenko, P. Prokopenko, A. Fomina, and V. Hauser, "Research of the strength of the bearing structure of the flat wagon body from round pipes during transportation on the railway ferry," *MATEC Web Conf.*, **235** (2018). doi:10.1051/matecconf/201823500003.
25) W. Fricke, "Fatigue analysis of welded joints: state of development," *Mar. Struct.*, **16** (*3*) 185–200 (2003). doi:10.1016/S0951-8339(02)00075-8.
26) M.E. Wiryawan, "Spesifikasi Teknis Gerbong Datar Kuat Muat 57 Ton (Technical Specifications of Strong Flat Carriage Loading 57 Tons)," 2020.
27) W.N. Putra, M.I. Adha Widjana, M. Anis, and Y. Prasetyo, "The effect of transformation temperature and holding time of bainite structure formation on s45c steel," *Evergreen*, **9**(*4*) 1218–1223 (2022). doi:10.5109/6625732.
28) J.I. Standard, "JIS (japanese industrial standards) g 3101. rolled steels for general structure," **2010** (2010).
29) J.I. Standard, "Revised in rolled steels for welded structure j i s g 3106-," (1999).
30) B.A. Kansake, "Multi-body dynamic and finite element modeling of ultra-large dump truck – haul road interactions for machine health and haul road structural integrity," 2019. https://scholarsmine.mst.edu/doctoral_dissertations.
31) S.A. Widyanto, O. Kurdi, G.D. Haryadi, I. Haryanto, and M.I. Rokhim, "Stress analysis of electric bus chassis using finite element method," *J. Phys. Conf. Ser.*, **1321** (*2*) (2019). doi:10.1088/1742-6596/1321/2/022014.
32) P. Štastniak, P. Kurčík, and A. Pavlík, "Design of a new railway wagon for intermodal transport with the adaptable loading platform," *MATEC Web Conf.*, **235** 4–8 (2018). doi:10.1051/matecconf/201823500030.
33) EN 12663-1:2010 (E), "Railway applications -Structural requirements of railway vehicle bodies - Part 1: Locomotives and passenger rolling stock (and alternative method for freight wagons)," 2010.
34) M. Spiryagin, A. George, S.S.N. Ahmad, K. Rathakrishnan, Y.Q. Sun, and C. Cole, "Wagon model acceptance procedure using australian standards," *Proc. Conf. Railw. Eng.*, (*October 2016*) 343–350 (2012).
35) V.M. Radhakrishnan, "Endurance diagram," *Int. J. Fatigue*, **12** (*6*) 513–517 (1990). doi:10.1016/0142-1123(90)90224-3.
36) Y. Aiman, S. Syahrullail, H. Hafishah, and M.N. Musa, "Friction characteristic study on flat surface embedded with micro pit," *Evergreen*, **8**(*2*) 304–309 (2021). doi:10.5109/4480707.
37) I.J. Maknun, and D.A. Aurellia Yasmiin, "Shear correction factor effect on functionally graded material (fgm) beam with timoshenko hencky beam (thb) element," *Evergreen*, **9**(*4*) 1210–1217 (2022). doi:10.5109/6625731.
38) K.S. Phad, and A. Hamilton, "Experimental investigation of friction coefficient and wear of sheet metals used for automobile chassis," *Evergreen*, **9**(*4*) 1067–1075 (2022). doi:10.5109/6625719.
39) R.G. Budynass, and J. Keith Nisbett, "Shigley's mechanical enineering design," *McGraw-Hill New York; 2011*, (n.d.).
40) S. Shrivastava, C. Ghosh, and J.J. Jonas, "A comparison of the von mises and hencky equivalent strains for use in simple shear experiments," *Philos. Mag.*, **92** (*7*) 779–786 (2012). doi:10.1080/14786435.2011.634848.
41) D. Skibicki, "Fatigue criterion based on the novoshilov criterion for non-proportional loadings," *Mater. Test.*, **53** (*6*) 327–331 (2011). doi:10.3139/120.110232.
42) M. Nowak, J. Ostorwska-Maciejewska, R.B. Pecherski, and P. Szeptynski, "Yield criterion accounting the third invariant of stress tensor deviator. part i. proposition of the yield criterion based on the concept of influence functions," *Eng. Trans.*, **59** (*4*) 273–281 (2011).
43) J.G. Da Silva, A.A. De Carvalho, and D.D. Da Silva, "A strain gauge tactile sensor for finger-mounted applications," *IEEE Trans. Instrum. Meas.*, **51** (*1*) 18–22 (2002). doi:10.1109/19.989890.
44) R.J.P.C. Miranda, P. Domingues, L.M. Zamboni, and J.C. Salamani, "The role of experimental stress analysis at graduation and post graduation courses - a brazilian case," *Appl. Mech. Mater.*, **24**–**25** 424–432 (2010). doi:10.4028/www.scientific.net/AMM.24-25.427.